# Probabilistic Risk Assessment on Maritime Spent Nuclear Fuel Transportation

Robby Christian [a], Hyun Gook Kang [b*]
[a,b]*KAIST, Nuclear & Quantum Eng. Dept., 291 Daehak-ro, Yuseong-gu, Daejeon 305-701*
[*]*Corresponding author: hyungook@kaist.ac.kr*

## 1. Introduction

Spent nuclear fuel (SNF) management has been an indispensable issue in South Korea [1]. Before a long-term SNF solution is implemented, there exists the need to distribute the spent fuel pool storage loads. Transportation of SNF assemblies from populated pools to vacant ones may preferably be done through the maritime mode since all nuclear power plants in South Korea are located at coastal sites. To determine its feasibility, it is necessary to assess risks of the maritime SNF transportation.

This work proposes a methodology to assess the risk arising from ship collisions during the transportation of SNF by sea. Its scope is limited to the damage probability of SNF packages given a collision event. The effect of transport parameters' variation to the package damage probability was investigated to obtain insights into possible ways to minimize risks. A reference vessel and transport cask are given in a case study to illustrate the methodology's application.

## 2. Methods

### *2.1. External Interaction*

The initial kinetic energy of ships on their course of collision is transformed into subsequent translation and rotation motions and the work done to deform ship structures and cargo. Let the frame of reference of ship collisions be as shown in Fig 1. The energy dissipated in the ξ when both ships stick together and when they slide against each other is given in Eq (1) and Eq (2) respectively [2].

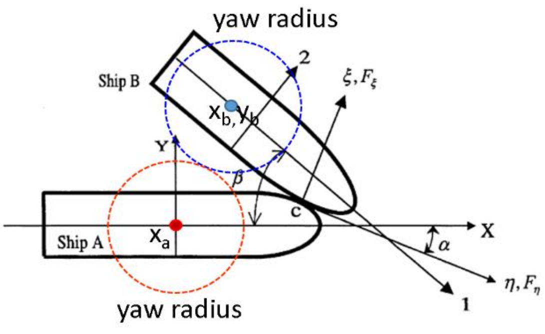


Fig 1. Coordinate system of ship collision

$$E_\xi = \int_0^{\xi_{max}} F_\xi d\xi = \frac{1}{2}\frac{1}{D_\xi + \mu \cdot D_\eta}\left(1-e^2\right)\left[\dot{\xi}(0)\right]^2 \quad (1)$$

$$E_\xi = \int_0^{\xi_{max}} F_\xi d\xi = \frac{1}{2}\frac{1}{D_\xi + \mu_0 \cdot D_\eta}\left(1-e^2\right)\left[\dot{\xi}(0)\right]^2 \quad (2)$$

A simplified triangular bow geometry was introduced to measure the impact location on the X-Y axis. With this geometry, collision scenarios are categorized as bow impact and side impact as shown in Fig 2. The impact location is therefore a function of the collision angle β and bow angle θ as given in Eq (3) and Eq (4). Conservative results are expected from the triangular bow compared to the rounded bow shape since the radius of inertia in side impact scenario is shorter.

$$x_c = L_A/2,\ y_c = 0 \,\Big|\, \theta/2 < |\alpha| < \pi - \theta/2 \quad (3)$$

$$x_c = \frac{1}{2}\left(L_A - \frac{B_A}{\tan\left(\theta/2\right)}\right), |y_c| = B_A/2 \quad (4)$$
$$\Big| \theta/2 \geq |\alpha|, \pi - \theta/2 \leq |\alpha|$$

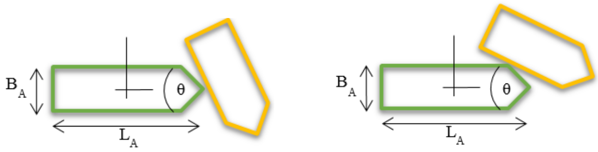


(a) Bow impact (b) Side impact

Fig 2. Impact locations

Transformations from the 1-2 axis to X-Y axis was done as illustrated in Fig 3. From the struck ship's perspective, the collision area of interest, i.e. the cargo hold area, in the local 1-2 coordinate system spans from $x_{cb\_min}$ to $x_{cb\_max}$. This area typically has a rectangular shape and therefore $|y_{cb}|$ at any point is a constant $B_A/2$. Additionally the angle α is equal to the collision angle β. The struck ship's center of mass in its local coordinate system is denoted as $x_{bb}$, a function of the ship's mass loadings. A set of translational and rotational equations to transform the struck ship's center of mass to the global coordinate system is given in Eq (5) until Eq (7).

$$x_{bb} = f(mass), y_{bb} = 0 \quad (5)$$

$$x_{bb}' = x_{bb} - x_{cb}, y_{bb}' = \pm\frac{B_B}{2} \quad (6)$$

$$\begin{bmatrix} x_b \\ y_b \end{bmatrix} = \begin{bmatrix} x_c & \cos(-\beta) & -\sin(-\beta) \\ y_c & \sin(-\beta) & \cos(-\beta) \end{bmatrix} \begin{bmatrix} 1 \\ x_{bb}' \\ y_{bb}' \end{bmatrix} \quad (7)$$

The struck ship's center of mass and radius of gyration depends on the mass loadings which include diesel fuel, oil, water ballast, crews, and the SNF cargo itself. The center of mass and radius of gyration are given in Eq (8) and Eq (9) respectively.

$$x_{bb} = \frac{\sum_i M_i \cdot x_{bi}}{\sum_i M_i} \tag{8}$$

$$R_b = \sqrt{\frac{\sum_i M_i \cdot x_{bi}^2}{\sum_i M_i}} \tag{9}$$

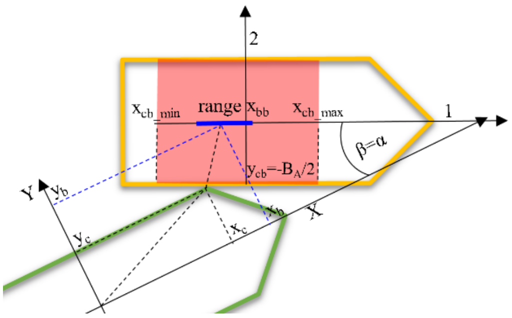


Fig 3. Coordinate transformation from SNF ship to striking ship

The impact energy is a function of the number and stowage of SNF transport casks onboard the struck vessel. Two stowage configurations with varying number of casks were investigated to obtain the risk's variation. In the aggregated stowage, casks are stowed in a hold to its maximum capacity before filling another hold. Meanwhile in the segregated stowage casks are distributed evenly in all holds. Additionally the direction of stowage was varied, i.e. from aft to bow and inversely from bow to aft.

### *2.2. Internal Mechanics*

The dissipated collision energy derived from the external interactions is used to crush struck ship's structure and SNF casks. Two cask impact scenarios termed frontal and side impact shown in Fig 4 may happen when striking ship penetrates deep enough into the cargo holds. This penetration distance was formulated as a function of the stress factor i.e. the collision energy, the strength of struck ship i.e. its penetration resistance and the geometrical likelihood of cask impact when collision happens.

The probability that transport casks are struck frontally is given by:

$$P_{cask\_bow} = \frac{B_{cask}}{L_B} \cdot \sum_{i=1}^{n_{loaded\_hulls}} n_{cask(i)} \cdot \iint_{x=x_d-B_{cask}/2,\, d=d_{min}}^{x=x_d+B_{cask}/2,\, d=B_B} P_{stress}(x).P_{strength}(x,d)\,\partial x \partial d \tag{10}$$

$$d_{min} = \frac{(B_B - L_{cask})}{2} \tag{11}$$

While the probability for a side-cask impact is given in Eq (12) to Eq (14):

$$P_{cask\_side} = \frac{L_H}{L_B} \cdot \frac{B_A}{n_{loaded\ hulls} \cdot L_H - n_{cask} \cdot B_{cask}} \cdot \iint_{x=x_d-s,\, d=d_{min}}^{x=x_d+s,\, d=B_b} P_{stress}(x) \cdot P_{strength}(x,d)\,\partial x \partial d \tag{12}$$

$$d_{\min} = s \cdot \cot(\frac{\theta}{2}) + \frac{B_B - L_{cask}}{2}, 0 < s < B_A/2 \tag{13}$$

If the collision is not perpendicular, i.e. α ≠ π/2, Eq (13) changes to Eq (14).

$$d_{\min} = \left| s.\cot(\frac{\theta}{2} \pm \left[\frac{\pi}{2} - \alpha\right]) \right| + \frac{B_B - L_{cask}}{2}, \quad 0 < s < \frac{B_A/2}{\sin(\theta/2)} \cdot \sin(\theta/2 \pm \left[\frac{\pi}{2} - \alpha\right]) \tag{14}$$

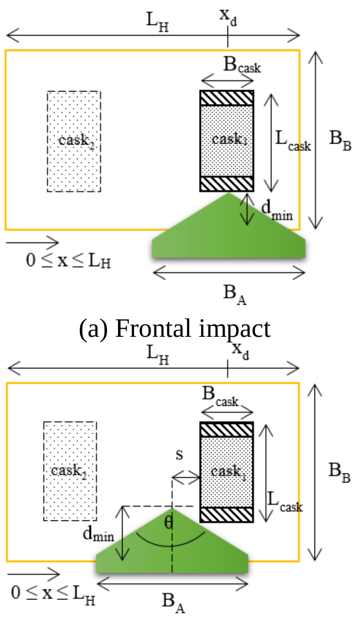


(a) Frontal impact

(b) Side impact

Fig 4. Transport cask impact scenarios

### *2.3. Reference Model*

Reference models of the SNF vessel and of the SNF transport cask are introduced to illustrate the difference in stowage configurations and to serve as a basis for the internal mechanics analysis. Properties of the SNF vessel are given in Table I.

Table I. SNF vessel's properties

| Name | Properties |
|---|---|
| Length Over All (LOA) | 80 m |
| Beam | 15.8 m |
| Draft | 4 m |
| Freeboard | 3.3 m |

| | |
|---|---|
| Cargo holds | 4, extending from LCG -9.6154 to 26.3846 m |
| Hold's length | 9 m |
| Net registered tonnage | 850 tonnes |
| Maximum velocity | 13 knots |
| Light ship weight | 2400 tonnes, LCG -3 m |

Dimensions of the transport cask are shown in Fig 5. Its capacity is 21 SNF assemblies. It weighs 100 tonnes when fully loaded and prepared for shipment. Based on the dimension and cargo capacity of the SNF ship, it can carry up to 8 transport casks where 2 casks can be fitted into a single cargo hold. Therefore the studied stowage configurations can be structured as given in Table II.

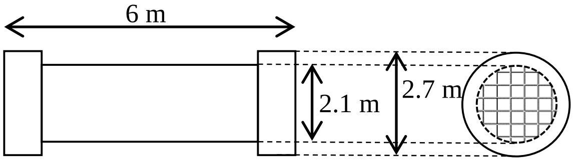


Fig 5. Reference model of the SNF transport cask

Table II. Transport cask stowage configurations

| Σ casks | Number of casks in each hold | | | | | | | |
|---|---|---|---|---|---|---|---|---|
| | Aft to bow direction | | | | | | | |
| | Segregated stowage | | | | Aggregated stowage | | | |
| | Hold #1 | Hold #2 | Hold #3 | Hold #4 | Hold #1 | Hold #2 | Hold #3 | Hold #4 |
| 1 | 1 | - | - | - | 1 | - | - | - |
| 2 | 1 | 1 | - | - | 2 | - | - | - |
| 3 | 1 | 1 | 1 | - | 2 | 1 | - | - |
| 4 | 1 | 1 | 1 | 1 | 2 | 2 | - | - |
| 5 | 2 | 1 | 1 | 1 | 2 | 2 | 1 | - |
| 6 | 2 | 2 | 1 | 1 | 2 | 2 | 2 | - |
| 7 | 2 | 2 | 2 | 1 | 2 | 2 | 2 | 1 |
| 8 | 2 | 2 | 2 | 2 | 2 | 2 | 2 | 2 |
| | Bow to aft direction | | | | | | | |
| 1 | - | - | - | 1 | - | - | - | 1 |
| 2 | - | - | 1 | 1 | - | - | - | 2 |
| 3 | - | 1 | 1 | 1 | - | - | 1 | 2 |
| 4 | 1 | 1 | 1 | 1 | - | - | 2 | 2 |
| 5 | 1 | 1 | 1 | 2 | - | 1 | 2 | 2 |
| 6 | 1 | 1 | 2 | 2 | - | 2 | 2 | 2 |
| 7 | 1 | 2 | 2 | 2 | 1 | 2 | 2 | 2 |
| 8 | 2 | 2 | 2 | 2 | 2 | 2 | 2 | 2 |

### *2.4. Nonlinear Finite Element Analysis*

Cargo holds of the struck ship were modelled with shell elements. Recommendations in reference studies [4, 5] were followed in defining the finite element type and size. The striking ship's bow section was conservatively assumed to be a rigid body having a mass of 2 x $10^5$ tonnes. Her breadth was 9.28 meters while her bow and draft angles were 53.13° and 30° respectively. This bow model collided with the cargo holds as shown in Fig 6 with an initial velocity of 15 knots.

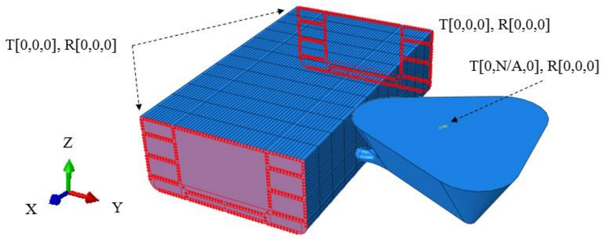


Fig 6. Collision simulation highlighting the boundary condition areas

## 3. Results

### *3.1. External Interactions*

Impact energy is dissipated in the ξ and η direction. However only $E_\xi$ determines the striking ship's depth of penetration into the struck ship. Fig 7 shows this impact energy and its maximum value when SNF ship was loaded to her maximum capacity of 8 SNF packages and was cruising at her maximum velocity of 13 knots. The energy peaked when the impact angle was 94° instead of 90° due to additional kinetic energy from the SNF ship. This peak energy was observed when ships stuck to each other during collision.

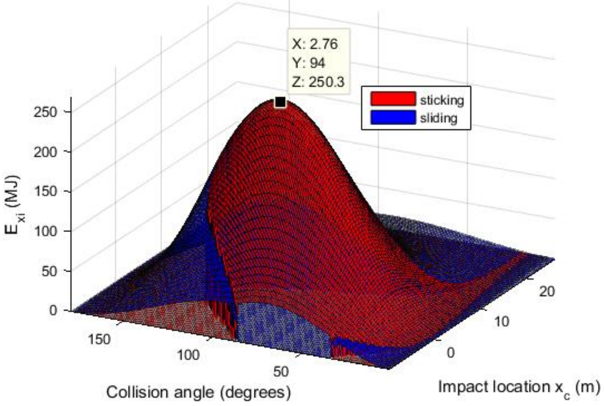


Fig 7. $E_\xi$ as a function of collision angle and impact location, given $V_B$=13 knots and $n_{cask}$=8

### *3.2. Internal Mechanics*

FEA result at the end of crush simulation is shown in Fig 8. The striking ship's loss of kinetic energy equals to the work required to breach through the SNF ship in the ξ direction from the point of impact. By varying this impact location, the overall strength of SNF ship was obtained. Combining the hold's strength profile with the transport cask locations and an impact energy when collision angle was 94° resulted in cask damage probability as depicted in Fig 9 (a). It shows that this collision penetrated deep enough into the hold to damage two transport casks. The proportion between side cask and frontal cask impact is highlighted in Fig 9(b). The cask damage probability was calculated as the range of impact locations leading to cask damage divided by the SNF ship's length which resulted in a value of 8.895 x $10^{-2}$.

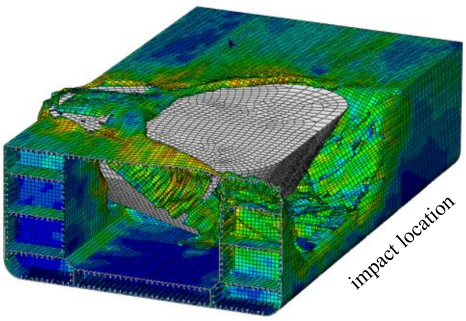


Fig 8. Sliced-view of crash simulation

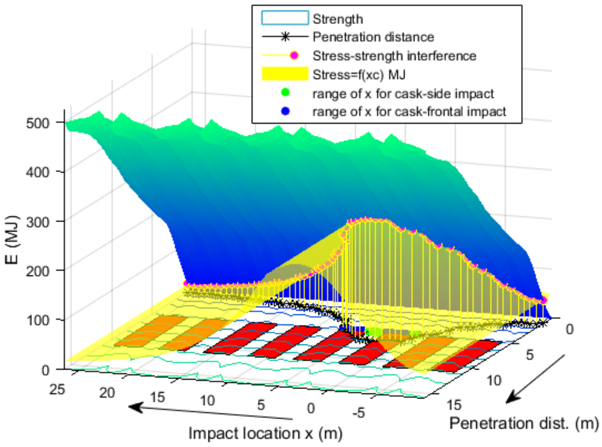


(a) $E_\xi$ and penetration distance from a collision at α=94° highlighting the positions of 8 transport casks

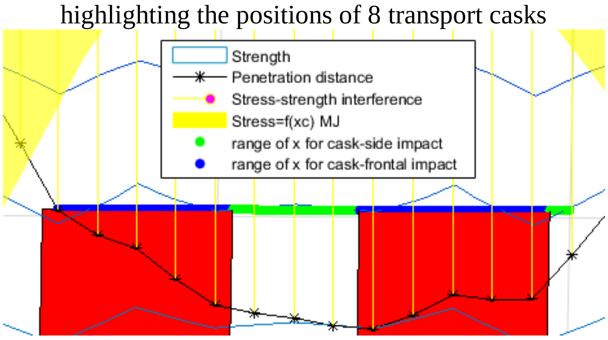


(b) Impact locations leading to frontal (blue line) and side cask impact (green line)

Fig 9. Cask damage probability from ship collision given $V_B$=13 knots, α=94° and $n_{cask}$=8

Fig 10 reveals the transport cask damage probability as a function of number of casks, stowage configuration, and SNF ship's velocity. Fig 10(a) compares cask damage probabilities when casks were segregated and loaded from aft-to-bow to the reversed order from bow-to-aft. The aft-to-bow loading direction gave higher probabilities compared to its counter direction. The maximum risk difference between these loading directions was observed when $n_{cask}$=6 where the risk difference varied from 7.7 x $10^{-3}$ to 9.4 x $10^{-3}$. Similarly, Fig 10(b) compares cask damage probabilities when casks were aggregated on the ship. The maximum risk difference was found when $n_{cask}$=4 where it varied between 4.7 x $10^{-3}$ and 9.5 x $10^{-3}$. These figures suggest that the optimal number of SNF packages to carry in a shipment was 4 out-of 8 stowed aggregately in the bow-to-aft loading order. This configuration ensures a satisfactory shipment rate while keeping the risk reasonably low.

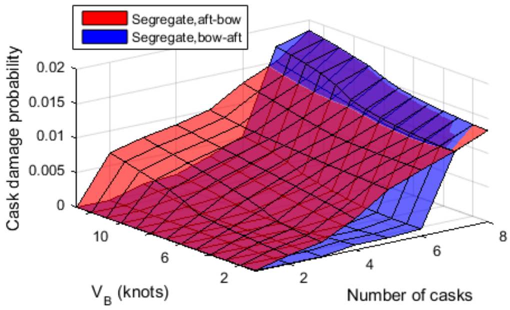


(a) Cask damage probability under the segregated stowage configuration

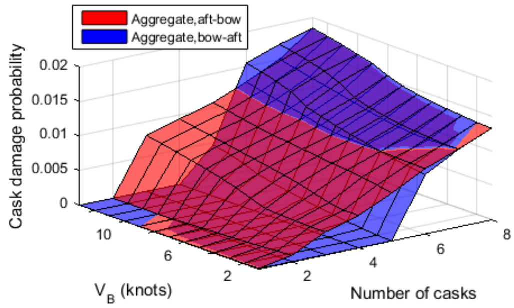


(b) Cask damage probability under the aggregated stowage configuration

Fig 10. Cask damage probability as a function of stowage configuration, number of transported casks and SNF ship's velocity

**ACKNOWLEDGEMENT**

This work was supported by the Nuclear Safety Research Program through the Korea Foundation Of Nuclear Safety(KOFONS), granted financial resource from the Nuclear Safety and Security Commission(NSSC), Republic of Korea (No. 1305032).

**REFERENCES**

[1] J.M. KANG, S.W. KIM, B.C. LEE, "Hot Potato in South Korea: The Spent Nuclear Fuel Storage Dilemma", Bulletin of the Atomic Scientists Vol 71(3), pp 76-83, 2015

[2] P.T. PEDERSEN, S. ZHANG, "On Impact Mechanics in Ship Collisions", Marine Structures 11, pp. 429-449, 1998

[3] J.F. SULLIVAN, "Technical Physics", John Wiley & Sons, 1988

[4] J.K. PAIK, J.H. PARK, E. SAMUELIDES, "Collision-Accidental Limit States Performance of Double Hull Oil Tanker Structures: Pre-CSR Versus CSR Design", Marine Technology Vol. 46, pp 183-191, 2009.

[5] P. HOGSTRÖM, J.W. RINGSBERG, "an Extensive Study of a Ship's Survivability after Collision – a Parameter Study of Material Characteristics, Non-Linear FEA and Damage Stability Analyses", Marine Structures, Vol. 27, pp. 1-28, 2012